Korean J. Chem. Eng., **30**(11), 2068-2077 (2013)
DOI: 10.1007/s11814-013-0148-y

Determination of cost-effective operating condition for CO_2 capturing using 1-butyl-3-methylimidazolium tetrafluoroborate ionic liquid

Emad Ali*,†, Inas Alnashef*, Abdelhamid Ajbar*, Sarwono Mulyono*, Hanee Farzana Hizaddin, and Mohamed Kamel Hadj-Kali***

*Chemical Engineering Department, King Saud University, P. O. Box 800, Riyadh 11421, Saudi Arabia
**Department of Chemical Engineering, University of Malaya, 50603, Kuala Lumpur, Malaysia
(*Received 24 April 2013 • accepted 5 August 2013*)

Abstract−1-Butyl-3-methylimidazolium tetrafluoroborate ([BMIM][BF4]) ionic liquid (IL) is considered for CO_2 capturing in a typical absorption/stripper process. The use of ionic liquids is considered to be cost-effective because it requires less energy for solvent recovery compared to other conventional processes. A mathematical model was developed for the process based on Peng-Robinson (PR) equation of state (EoS). The model was validated with experimental data for CO_2 solubility in [BMIM][BF4]. The model is utilized to study the sorbent effect and energy demand for selected operating pressure at specific CO_2 capturing rates. The energy demand is expressed by the vapor-liquid equilibrium temperature necessary to remove the captured CO_2 from the spent solvent in the regeneration step. It is found that low recovery temperature can be achieved at specific pressure combination for the absorber/stripper units. In fact, the temperature requirement is less than that required by the typical monoethanolamine (MEA) solvent. The effect of the CO_2 loading in the sorbent stream on the process performance is also examined.

Key words: Ionic Liquid, CO_2 Solubility, CO_2 Capturing, PR Equation of State

INTRODUCTION

It is widely accepted that global warming is occurring. Many scientists believe that the major cause is the emission of greenhouse gases (GHGs), such as carbon dioxide (CO_2), nitrous oxide and methane, into the atmosphere. Among these GHGs, CO_2 is the largest contributor in regard to its amount present in the atmosphere, contributing about 60% of global warming effects [1]. Consequently, CO_2 capture and sequestration from fossil-fueled power plants is drawing increasing attention as a potential method for controlling greenhouse gases emissions. Among different developed methods, post-combustion capture has the advantage that it can be applied to retrofit the existing power plants. The most mature technology for CO_2 post-combustion is amine-based absorption due to the high affinity of amines (MEA, MDEA and DEA) to CO_2 [2-7]. However, the solvent recovery in this process for reuse becomes very expensive in terms of energy requirements since the amine-based absorption belongs to the chemical separation methods which demand intensive energy to break the chemical bonds between the absorbents and the absorbed CO_2 in the regeneration step [8,9]. Therefore, it is beneficial to find alternative solvents that combine high affinity for CO_2 with easier solvent regeneration and reuse.

Ionic liquids have emerged as promising alternatives and have gained increasing attention as highly potential candidates to replace amine-based solvents when Blanchard et al. discovered the high solubility of CO_2 in ionic liquids [10]. Ionic liquids are molten salts, liquid at room temperature, that consist of a combination of asymmetrical large-sized cations with smaller, more symmetric anions.

†To whom correspondence should be addressed.
E-mail: amkamal@ksu.edu.sa

Ionic Liquids have several advantages, including (i) negligible vapor pressure, which leads to zero emission of volatile organic compounds, (ii) high thermal and chemical stability, which leads to ionic liquids having a wide liquidus range, and (iii) non-flammability. They are also known as 'designer solvents', originating from several combinations of cations and anions, tunable for a specific application. Another relevant advantage for our specific purpose is the low energy demand to extract the absorbed CO_2 from ILs in the regeneration step, which is attributed to a physical absorption mechanism [11].

In this work, numerical simulations are performed to study the CO_2 capture using conventional 1-butyl-3-methylimidazolium tetrafluoroborate [BMIM][BF4] ionic liquid. It is widely accepted that the anion of the ionic liquids has a greater influence towards CO_2 solubility in ILs, while the role of the cation is secondary [12]. The solubility of CO_2 in [BMIM]-based ionic liquids with different anions increases in the order $[NO_3]^-$<[DCA]$^-$<[BF4]$^-$<[PF6]$^-$<$[CF_3SO_3]^-$<$[Tf_2N]^-$<[methide]$^-$ [13]. Kazarian et al. reported in situ ATR-IR spectroscopy data which discovered that the anions [BF4] and [PF6] have favorable interaction with CO_2 [14]. Moreover, Jacquemin et al. [15] reported solubilities of several gases in [BMIM][BF4] at low pressure. It was found that the solubility of gases follows the order of H_2<CO<N_2<O_2<Ar<CH_4<C_2H_6<CO_2 with CO_2 having the highest solubility, and thus highest selectivity against other gases.

Therefore, even though other ionic liquids have shown better CO_2 solubility, the selection of [BMIM][BF4] for this study was motivated by (i) the rich database of consistent experimental results available in the literature, (ii) its high selectivity for CO_2 as well as (iii) its ease of synthesis, and (iv) its relatively low price in comparison to other ILs.

The solubility of CO_2 is determined using the homogeneous approach based on the PR EoS. Using the developed model, paramet-

ric estimation study is performed to compare the energy requirements for the process through investigating the effects of stripper operating temperature, CO_2 removal percentage, the CO_2 lean solvent loading and the rich solvent loading. The thermodynamic model, which is the core of the process, is used to estimate the equilibrium constant and vapor-liquid equilibrium necessary to carry out the parametric study.

Many researchers have used The PR EoS to estimate the vapor-liquid equilibrium (VLE) [16]. This equation is suitable to handle systems containing hydrocarbons, water, air and combustion gases, the typical components in a natural gas based power plant. Other applications to mixtures containing CO_2 are reported. Harvey [17] used the PR EoS for VLE calculation for water with synthesis gas mixtures. Tombokan [18] reported successful application for polar

Table 1. Summary of previous publications where the Peng-Robinson EoS was used with ionic liquids systems

EoS/Mixing rule/Activity Coefficient Model	System	T range (K)	P range (MPa)	Reference
Generic RK EOS+empirical function for "a"+modified vdW-Berthelot mixing rule	CO_2+[C_4mim][PF_6] CO_2+ [C_4mim][BF_4]	283-348	Up to 2	[17]
PR/Wong-Sandler/UNIQUAC	CO_2 & CHF3 & hydrocarbons in ILs ([C_4mim][PF_6], [C_4mim][NO_3] [C_4mim][BF_4]	298-333	0.8-64	[20]
PR/Wong-Sandler/UNIQUAC	CO_2+[C_2mim][bti] CO_2+[C_5mim][bti]	293-363	0.6-50	[21]
PR/Wong-Sandler/UNIQUAC	CO_2+[C_4mim][bti] CO_2+[C_4mim][DCA]	293-363	0.6-50	[22]
PR/Wong-Sandler/van Laar	CO_2+[C_4mim][NO_3], [C_4mim][BF_4], [C_4mim][DCA], [C_4mim][TfO], [C_4mim][methide], [C_4mim][bti], [C_6mim][bti], [C_8mim][bti]	313 & 333	1.2-12	[23]
PR/Wong-Sandler/NRTL	CO_2 with N-methyl-2-hydroxyethylammonium formate and N-methyl-2-hydroxyethylammonium acetate	293-353	Up to 80	[24]
Peng-Robinson/Stryjec-Vera EoS/ Wong-Sandler/van Laar	17 binary mixtures of ionic liquid+gas	298-363	Up to 97	[26]
PR-Kwok Mansoori	CO_2 with either [C_8mim][PF_6], [C_2mim][$EtSO_4$], [C_6mim][bti], [C_8mim][BF_4], [C_4mim][PF_6], [C_4mim][NO_3]	313-323	14-97	[25]
PR+van der Waals 2-parameter mixing rule	CO_2+C_2mim[bti] CO_2+C_6mim[bti] CO_2+C_{10}mim[bti]	298-345	1.2-15	[27]
PR+van der Waals mixing rule	CO_2+[C_8mpyr][bti] CO_2+[C_8mpyr][bti]	303-373	0.5-48	[28]
Peng-Robinson equation of state along with two-parameter mixing rules	CO_2+[$C_n$mim][BF_4]	293-323	2-10	[29]
PR and quadratic mixing rule with parameters a and b modified by Adachi and Sugie	CHF_3 in ILs			[30]
PR with quadratic mixing rule	CO_2+[$C_n$mim][bti]	298-368	Up to 45	[31]
PR with quadratic mixing rule	CO_2+[BMP][TfO], ([P14,6,6,6]-[bti]	303-373	Up to 70	[32]
PR with quadratic mixing rule	CO_2+C_4mim[Cl]	353-373	Up to 40	[33]
PR/van der Waals one-fluid mixing rule	R-134a in [C_6mim][bti], [C_6mim][PF_6], [C_6mim][BF_4], [C_6m][bti]	298-373	Up to 14.3	[34]
PR/van der Waals one-fluid mixing rule	CO_2, 1-bromohexane, 1-methylimidazole and 1-hexyl-3-methylimidazolium bromide ([C_6mim][Br]	313 & 333	1 -16	[35]
PPR78	N_2O+[C_4mim][BF_4], [C4mim] [SCN], [C_{10}mim][MP], [(OH)2IM][bti]	293-373	Up to 30	[36]
PPR78	CO_2+[C_4mim] [BF_4], [C_4mim] [SCN], [C_{10}mim] [MP], [(ETO)2IM][bti]	293-373	Up to 30	[37]
PR with Mathias-Klotz-Prausnitz mixing rule, SRK with Mathias-Klotz-Prausnitz mixing rule	CO_2+1-propanol+C_2mim[bti], CO_2+1-propanol +C_{10}mim[bti], CO_2+1-propanol+C_2mim[tfo], CO_2+C_{10}mim[bti]	313	Up to 14	[38]

systems, systems containing gases (CO_2, CH_4 and C_2H_6) with n-alkanes, sterols and vitamins in CO_2. Greer [19] also utilized PR EoS to estimate the VLE for CO_2-MEA mixtures in order to design the CO_2 absorber column. Similar effort was also reported by Lars [20].

In 2005, Shiflett and Yokozeki claimed to be the first to use a cubic equation of states to model CO_2 solubility in ionic liquid [21]. They used a generic Redlich-Kwong (RK) EoS with an empirical function of the parameter 'a' and modified van der Waals-Berthelot mixing rule to model CO_2 solubility in two imidazolium-based ionic liquids. They predicted the phase behavior, Henry's constant and volume change of solutions.

Moreover, the PR thermodynamic model is well tested with extensive experimental data and has been used successfully in VLE representation of many systems involving ionic liquids. Maia et al. [22] did a comprehensive review on the use of various equations of state to describe the behavior of CO_2 and other gases in ionic liquids. Earlier in 2010, Vega et al. [23] also published a review on the modeling works used to describe solubility of gases in ionic liquids. Table 1 shows a summary of previous works where the PR EoS was used to model solubility of CO_2 in various ionic liquids at different temperature and pressure ranges with the mixing rules and/or activity coefficient models used in each references.

As can be seen in this table, the PR EoS is most frequently used in modeling the CO_2-IL systems combined with different mixing rules and either with or without activity coefficient models. Alvarez and Aznar [24] were the first to use the combination of PR EoS with Wong-Sandler mixing rule and UNIQUAC model to model CO_2 and other gases solubility in ionic liquids with the purpose of performing a consistency test. Later, Carvalho et al. [25,26] adopted the same combination of EoS/mixing rule/activity coefficient model to perform a consistency test on systems with CO_2 and imidazolium-based ionic liquids at pressures up to 50 MPa.

On the other hand, Valderrama et al. [27] developed another approach for performing a consistency test for systems with CO_2 and ionic liquids, but this time with a combination of PR EoS with Wong-Sandler mixing rule and van Laar model. Later in 2011, Mattedi et al. [28] adopted the combination of PR EoS with Wong-Sandler mixing rule and NRTL model to describe the solubility of CO_2 in ammonium-based ionic liquids. Recently, Valderrama et al. [29] used PR EoS with the Kwak-Mansoori mixing rule to model CO_2 solubility in imidazolium-based ionic liquids, and the results of the modeling are compared against using different combinations of equation of state, mixing rules and activity coefficient models. Arce et al. [30] described 17 binary mixtures of gases and ionic liquids using another variation of PR EoS, named Peng-Robinson/Stryjec Vera (PRSV) EoS where the Wong-Sandler mixing rule and van Laar model were coupled.

PR EoS can also be used without the combination with activity coefficient models to describe solubility of CO_2 and other gases in ionic liquids. Ren et al. [31], Yim et al. [32] and Hwang et al. [33] each used the PR EoS with van der Waals mixing rule to describe solubility of CO_2 in ionic liquids. Shariati and Peters [34] used PR EoS with quadratic mixing rule to describe the solubility of fluoroform in ionic liquids. Similar combination was also adopted to describe solubility of CO_2 in ionic liquids by Shin et al. [35], Song et al. [36] and Jang et al. [37]. Meanwhile, Ren and Scurto [38] and Nwosu et al. [39] used PR EoS with van der Waals one-fluid mixing rule to describe the solubility of the refrigerant R0134a and CO_2 in ionic liquids, respectively.

Revelli et al. [40,41] used the Predictive Peng-Robinson EoS (PPR78) to describe the solubility of nitrous oxide and CO_2 in ionic liquids, respectively. Bogel-Lukasik et al. [42] described binary and ternary systems of CO_2 and 1-propanol in ionic liquids by using both the PR and Soave-Redlich-Kwong (SRK) EoSs with Mathias-Klotz-Prausnitz mixing rule.

Thus, it can be safely concluded that the PR EoS is widely used to describe mixtures of CO_2 with ionic liquids.

THE ABSORBER MODEL

A schematic description of the CO_2 capturing process is depicted in Fig. 1. The process consists of an absorber followed by a stripper. In the absorber, the lean sorbent is fed to extract the CO_2 in the flue gas. The contaminated sorbent is then sent to the stripper for regeneration where the exact amount of CO_2 captured is assumed to be released in the top product. The regenerated solvent is recycled back to the absorber. In this work the stripper is treated as a simple flash drum where it is assumed that the required amount of CO_2 to be released occurs at a specific VLE condition. The flue gas is mainly air with some amount of CO_2 and water vapor. It is assumed that only CO_2 is miscible in the solvent and that transfer of liquid species to the gas phase is negligible. The CO_2 transfer to the liquid phase is only due to physical absorption--no chemical reaction occurs.

The absorber is a multistage countercurrent column as shown in Fig. 2. Assuming steady state and adiabatic conditions, the typical component balance for stage i is given as follows:

$$G_{i+1}y_{i+1}+L_{i-1}x_{i-1}=G_iy_i+L_ix_i \tag{1}$$

In terms of inert free flow rates, which is valid since only CO_2 is transferring,

$$G\frac{y_{i+1}}{1-y_{i+1}}+L\frac{x_{i-1}}{1-x_{i-1}}=G\frac{y_i}{1-y_i}+L\frac{x_i}{1-x_i} \tag{2}$$

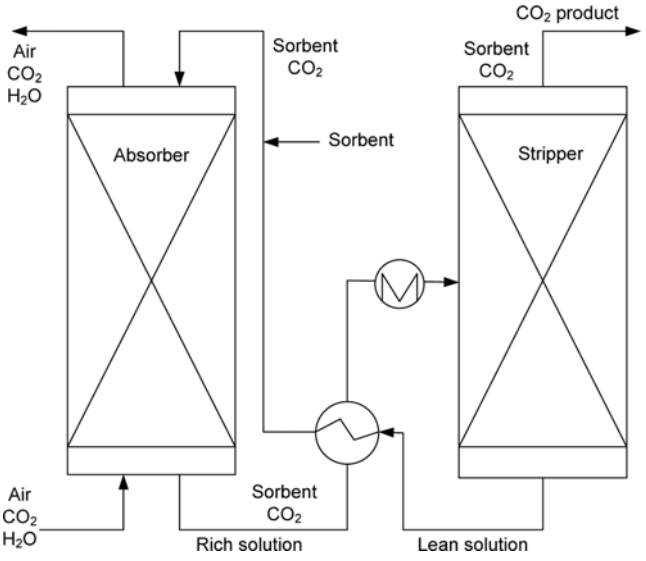

Fig. 1. Schematic of the CO_2 capturing process.

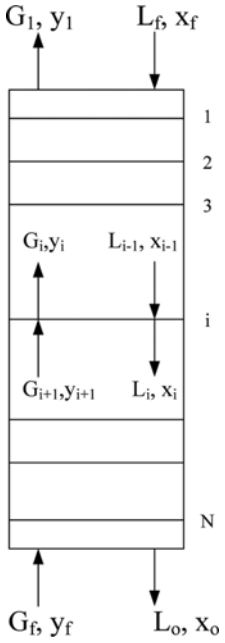

Fig. 2. The absorber column.

The equilibrium line is:

$$y_i = K_i x_i \tag{3}$$

The gas feed conditions are well defined. Specifically, the feed flow rate is taken to be 12,000 mol/h, with 5% CO_2, 1% water vapor and the rest is air. CO_2 removal efficiency will be taken to be 0.85. These operating conditions are within the range used in literature [5,6,19]. Therefore, given the CO_2 removal efficiency and assuming that only CO_2 is absorbed by the liquid phase, the gas outlet condition can be exactly determined using the overall mass and component balances. Since the component mole fraction in the gas phase is related to the liquid phase via Eq. (3) and since the end conditions of the gas feed are known, the remaining unknown variables are the liquid phase mole fractions and the solvent flow, L. In this case, the number of unknown variables is N+1. Because N component material balance equations can be written, an additional given relation must be defined. The equilibrium constant, K_i in (3) will be determined via VLE analysis as described in the next section.

THE THERMODYNAMIC MODEL

When a liquid mixture is in equilibrium with its vapor at fixed temperature and pressure, the thermodynamic equilibrium is expressed by the equality of the fugacity f in both the liquid and vapor phases for every component i:

$$\hat{f}_i^L = \hat{f}_i^V, \quad i=1, \cdots, nc \tag{4}$$

The homogeneous approach ($\phi-\phi$ method) was adopted to calculate the fugacities for each component in both liquid and vapor phases as follows:

$$\hat{f}_i^L = x_i \phi_i^L P, \quad \hat{f}_i^V = y_i \phi_i^V P \tag{5}$$

The VLE calculation in this case is an iterative procedure where the liquid and vapor mole fraction are determined at fixed temperature and pressure such that the condition in (4) in addition to the following conditions,

$$\sum_{i=1}^{nc} x_i = 1, \quad \sum_{i=1}^{nc} y_i = 1 \tag{6}$$

is satisfied. Once the VLE is satisfied, the CO_2 solubility in the specific IL is taken as its mole fraction in the liquid phase, i.e. x_{CO2}.

Mixing rules are required to calculate A and B (from a and b) and extend the application field of equation of state to mixtures. In this work, the classical mixing rule of the van der Waals was used:

$$A = \sum_{i=1}^{nc}\sum_{j=1}^{nc} y_i y_j \sqrt{A_i A_j}(1-k_{ij}), \quad B = \sum_{i=1}^{nc} y_i B_i \tag{7}$$

where k_{ij} is the binary interaction parameter adjustable to fit the experimental VLE data.

CO_2 can be physically absorbed in a solvent according to Henry's law, applicable to gases with high partial pressure. The solvent regeneration step is relatively simple for physical absorption as it is carried out by decreasing the pressure. In this work, the solubility of CO_2 in 1-butyl-3-methylimidazolium tetrafluoroborate is determined by the VLE analysis using the PR EoS defined by the general expression [43,44]:

$$P = \frac{RT}{v-b} - \frac{a}{v(v+b)+b(v-b)} \tag{8}$$

where a, and b are a function of the critical properties of the chemical species. The properties of CO_2 and 1-butyl-3-methylimidazolium tetrafluoroborate required for the calculation are listed in Table 2. Data for CO_2 are taken from the ASPEN database, while for ionic liquids the estimated pseudo-critical properties are taken from the work of Valderrama et al. [45] who developed a group contribution method to obtain these properties.

By introducing the compressibility factor, Z=Pv/RT, Eq. (8) can be rearranged into a cubic equation and solved numerically at fixed temperature and pressure to obtain the component fugacity coefficient for each phase [43]:

$$\phi_i = \exp\left[(Z-1)\frac{B_i}{B} - \ln(Z-B) - \frac{A}{2\sqrt{2}B}\left(\frac{2\sum_j y_i A_{ij}}{A} - \frac{B_i}{B}\right)\ln\left(\frac{Z+(1+\sqrt{2})B}{Z-(1-\sqrt{2})B}\right)\right] \tag{9}$$

Where $A_i = \frac{a_i P}{(RT)^2}$, $B_i = \frac{b_i P}{RT}$

After solving the above Eq. (5), the largest and smallest roots of the cubic equation are used to compute the vapor and liquid phase fugacities, respectively. The mixing rule used in Eq. (5) includes the binary interaction parameters to account for mismatch between the experimental values and the model predictions. For binary mix-

Table 2. Pure component properties of CO_2 and 1-butyl-3-methylimidazolium tetrafluoroborate

Component	T_c (K)	P_c (atm)	ω
[BMIM][BF4]	632.3	20.4	0.8489
CO_2	304.2	73.8	0.224

ture like the one handled in this paper, this parameter reduces to a single variable. It is optimized in this work with experimental data found in the literature. In due course the solubility prediction is cast as an optimization problem. The following optimization will be considered here as follows:

$$\min_{x_i,y_i,k_{ij}} \phi=(x_{CO_2}-x_s)^2 \quad (10)$$

The objective function is subject to constraints represented by Eqs. (5) and (6). In Eq. (10), x_i and y_i are the component mole fraction in the liquid and gas phase, respectively; x_s is the experimental value for CO_2 solubility in the liquid salt.

Validation of the solubility of CO_2 in 1-butyl-3-methylimidazolium tetrafluoroborate against experimental data is shown in Fig. 3. The experimental data is taken from [15]. The entire VLE calculation is carried out using MATLAB software. Extrapolation of the validated thermodynamic model to estimate the CO_2 solubility at selected temperature and pressure is shown in Figs. 4 and 5. Both figures show reasonable trends as the solubility increases with increasing the pressure and/or decreasing the temperature of the mixture.

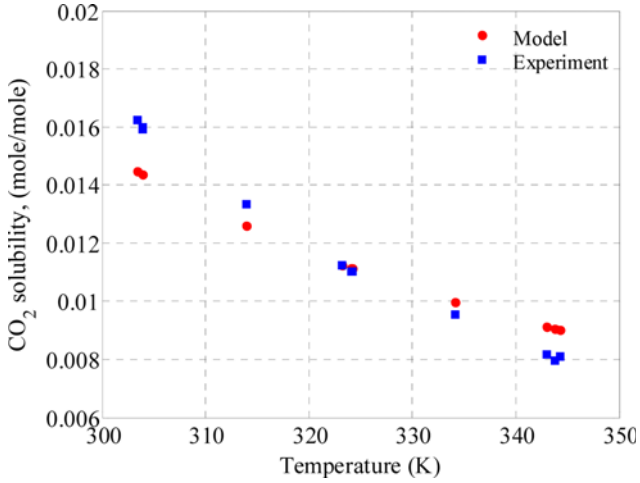

Fig. 3. Validation of the PR Eos model against experimental data.

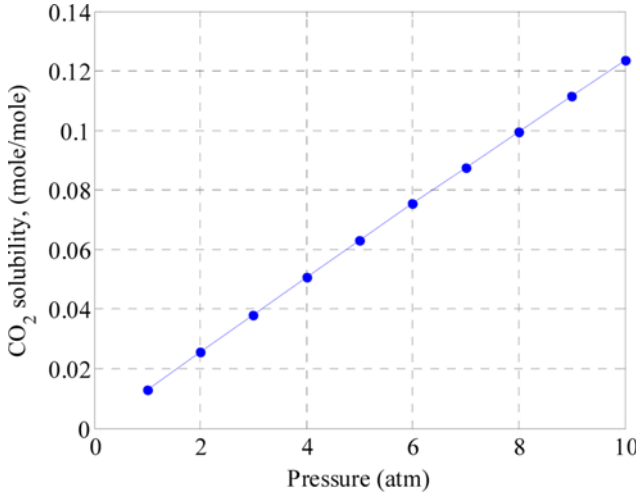

Fig. 4. Variation of CO_2 solubility in 1-butyl-3-methylimidazolium tetrafluoroborate with selected pressures at 40 °C.

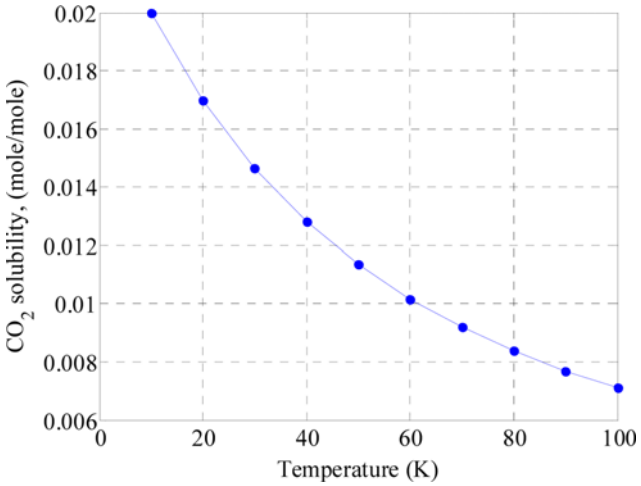

Fig. 5. Temperature effect on CO_2 solubility in 1-butyl-3-methylimidazolium tetrafluoroborate at 1 atm.

THE STRIPPER MODEL

The PR equation of state is further utilized in this work to carry out flash calculation for the flash drum which is assumed to represent the stripper unit. The flash calculation involves determining the vessel temperature and the corresponding equilibrium liquid and vapor composition at fixed pressure and given feed conditions. Moreover, the calculation will determine the portion of the feed that vaporized. This is another numerical iteration that involves satisfying the conditions set by Eqs. (4) (5) and (6) in addition to the Rachford-Rice equation:

$$\sum_{i=1}^{nc}\frac{z_i(K_i-1)}{1+\lambda(K_i-1)}=0 \quad (10)$$

where z_i is the mole fraction of the stripper feed, $K_i=y_i/x_i$ is the equilibrium constant, and λ is the molar ratio of the produced vapor to the feed.

To ensure that the amount of CO_2 extracted in the flash drum equals exactly the amount captured in the absorber column, the following constraint is also added to the flash calculations:

$$\lambda F y_{CO_2}-CO_{cap}=0 \quad (11)$$

where F is the molar flow rate of the flash feed (rich solution), y_{CO_2} is the mole fraction of CO_2 in the vapor flow rate (CO_2 product), and the CO_{cap} is the amount of CO_2 captured in the absorber column. The purpose of the flash calculation is to determine the energy requirement for regenerating the solvent in terms of the flashing temperature. Therefore, the temperature will be a measure of the cost effectiveness of the IL used for CO_2 capturing. The energy requirement for regeneration is based only on overcoming the physical absorption, i.e., to vaporize specific amount of the CO_2 in the rich solution. This means that the energy required to overcome the chemical reaction, if any, is not considered. The entire numerical flash calculations were carried out using MATLAB software.

RESULTS AND DISCUSSION

The given IL has different levels for CO_2 solubility with respect

to the temperature and pressure as shown in Figs. 4 and 5; consequently, it will have different effect on the CO_2 capturing process. It is believed that higher solubility will consume less sorbent. However, the energy required to extract the CO_2 from the rich sorbent in the desorption column will be higher. The effect of the process operating pressure and temperature to reverse the absorption was examined to determine the most economical operating condition. First CO_2 is captured in the absorption column at specific pressure and then the operation is reversed at the stripping column by either lowering the pressure or increasing the temperature. The simultaneous effect of the pressure of both units, i.e., the absorber and the stripper columns, was investigated.

To solve the absorber mass balance equations, one degree of freedom should be specified. In this work, we have examined three cases: (i) fixing the CO_2 mole fraction in the absorber outlet stream (rich sorbent effluent), x_o, (ii) fixing the CO_2 mole fraction in the absorber feed (lean sorbent influent), x_f, and finally (iii) fixing the sorbent flow rate, L.

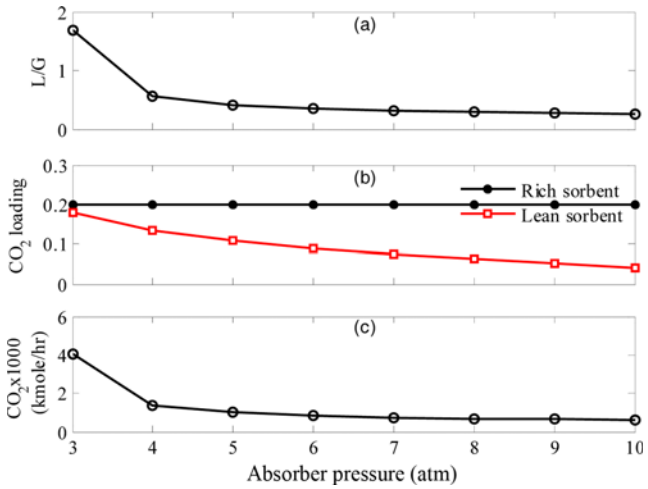

Fig. 6. Effect of pressure on the absorption rate at x_o=0.2, f=85%, T=25 °C.

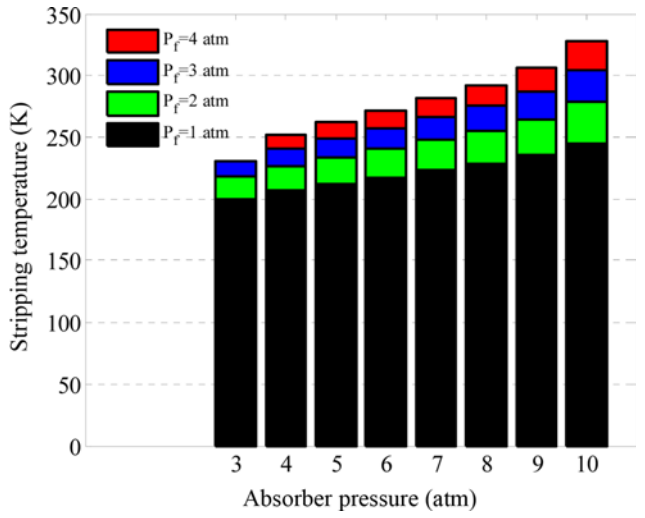

Fig. 7. Effect of absorber and stripper pressure on the recovery temperature at x_o=0.2 and f=85%.

For the first case, the CO_2 loading in the rich sorbent was fixed at x_o=0.2 and 0.3. Figs. 6 and 7 illustrate the simulation results for the case when x_o is set to 0.2. In fact, the absorber model (Eqs. (1) to (3)) is solved at various pressure values with x_o=0.2, T=25 °C and CO_2 to determine the corresponding sorbent flow rate and the CO_2 loading in the leans solvent stream. The equilibrium constant (K) required by the absorber model is determined by the VLE model at the specified temperature and pressure. Fig. 6 depicts the effect of increasing the absorber pressure. As the pressure increases, CO_2 solubility in the IL increases leading to less demand for the sorbent flow rate. At low pressure of 3 atm, the sorbent demand grows substantially as the CO_2 loading in the lean solvent stream approaches that of the rich stream. Numerical solution of the absorber model below 3 atm is not feasible because it requires x_f to exceed x_o, which is physically impossible. In fact, it is reported in [6] that the operating pressure of the absorber column should be more than 9 atm for CO_2 capturing by physical absorption. Fig. 7 shows the effect of the absorber and stripper pressure on the flash temperature required to release exactly the same amount captured in the absorber column. Note that the stripper pressure could be equal or less than the absorber pressure. It is obvious and logical that increasing the stripper column pressure requires higher temperature for the specified separation. Similarly, using high pressure on the absorber column will affect the separation temperature at the stripper stage. The effect is indirect, which is caused by the condition of the stripper feed. By inspecting Fig. 6, it can be seen that at higher absorber pressure the sorbent flow contains less amount of CO_2 than that at low pressure. Consequently, the amount of CO_2 to be released which is equivalent to that captured upstream becomes a large portion of the rich sorbent stream, i.e., the stripper feed flow. Therefore, higher energy is needed to spate larger ratio of the stripper feed. On the other hand, as indicated by Fig. 7 very low temperature is required to recover the captured CO_2 because its amount becomes very small compared to the total amount of CO_2 in the sorbent stream. It should be clear that the amount of CO_2 to be recovered from the rich solvent in the stripper is different than the total amount of CO_2 in the same stream. The amount to be recovered is fixed to the amount captured in the absorber column regardless of the absorber and/or stripper operating pressure. Moreover, the considerable amount of CO_2 at low absorber pressure should not be confused by the solubility factor. It is true that at low pressure the solubility decreases hindering the solvent stream from attracting more CO_2. However, the large amount of CO_2 at low pressure is due to the propagated amount of solvent flow. Nevertheless, operating the absorber column below 5 atm is undesirable because it requires huge solvent flow and very low separation temperature, which is physically unacceptable although it is numerically feasible. In conclusion, Fig. 7 indicates that in order to operate the process around moderate separation temperature of 300 K to avoid the excessive energy required by the MEA process, the absorber column should operate around 9 or 10 atm and the stripper at least at 3 atm.

To study the effect of the CO_2 loading in the rich sorbent on the process behavior, the above simulation is repeated with x_o being fixed at 0.3. The result is shown in Fig. 8. It is found that using higher value for x_o allows for lower value for the absorber pressure as much as 2 atm. However, unrealistic operation is still observed at low column pressure in Fig. 9, i.e., very low separation temperature, high

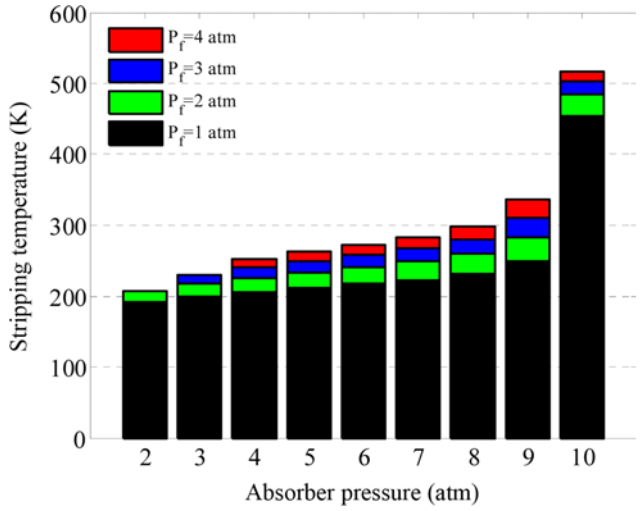

Fig. 8. Effect of absorber and stripper pressure on the recovery temperature at x_o=0.3 and f=85%.

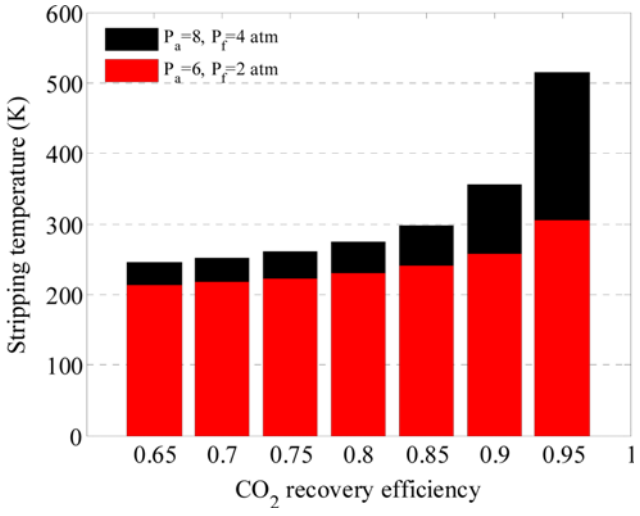

Fig. 10. Effect of CO_2 recovery efficiency on the stripping temperature when x_o=0.3.

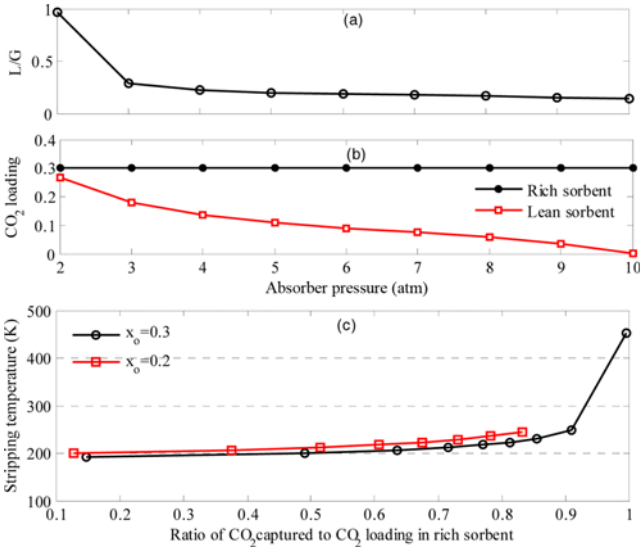

Fig. 9. Comparison of stripping temperature for x_o=0.3 and 0.2 at P_f=1 atm and f=85%.

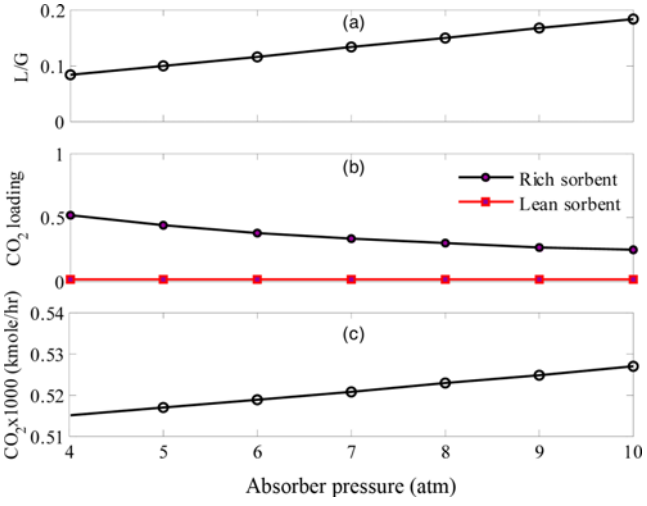

Fig. 11. Effect of pressure on the absorption rate at x_f=0.01, f=85%, T=25 °C.

solvent demand and large CO_2 content in the absorber effluent. The latter is not shown here for brevity. Interestingly, the required stripping temperature is lower than that obtained for x_o=0.2 except at 10 atm, where a sudden jump is observed. Moreover, the flashing temperature at that case is much higher than that reported for x_o= 0.2. The larger temperature demand is attributed to the CO_2 content in the stripper feed flow rate (rich sorbent) as confirmed in Fig. 9(c). The figure compares the stripping temperature for the above two cases when the stripper pressure is fixed at 1 atm. Similar results can also be shown for the other operating pressures. In this diagram (Fig. 9), the stripping temperature shown in Figs. 8 and 7 are replotted against the ratio of the CO_2 to be removed to the total CO_2 in the rich sorbent flow instead of the absorber pressure. Hence, Fig. 9(c) indicates that for x_o=0.3, the CO_2 content in the rich sorbent at P_a=10 atm becomes very small and almost equal to the amount to be removed. This explains why much high flashing temperature is needed.

The above analysis was carried out at fixed CO_2 removal efficiency of 0.85. It is interesting to study the process behavior at different levels of removal capacities. Fig. 10 shows this behavior. It is obvious that the required separation temperature increases when higher efficiency is required. For example, 95% removal capacity may necessitate considerable energy as the flashing temperature approaches 500 K. Therefore, to reduce the energy requirement at high removal efficiency one can consider operating at lower operating pressure. Fig. 9 shows that at P_a=6 atm and P_f=4 atm, 95% efficiency can be achieved at stripping temperature as low as 300 K.

Next, we examined simulating the process for fixed CO_2 loading in the lean solvent. In this case, x_f will be held at 0.01 and the absorber and stripper models along with the thermodynamic model are numerically solved for f=85% and different values of pressure to determine the solvent flow rate (L), rich sorbent loading (x_o) and the required flashing temperature. Figs. 11 and 12 illustrate the outcome of such simulation. In due course, remarkable results are ob-

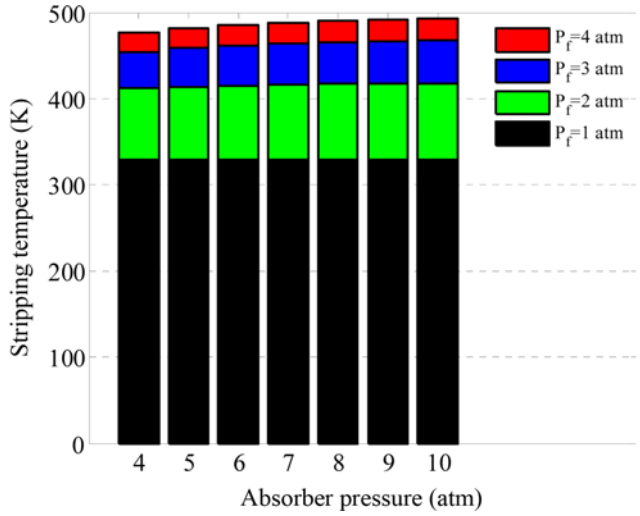

Fig. 12. Effect of absorber and stripper pressure on the recovery temperature at x_f=0.01, f=85%.

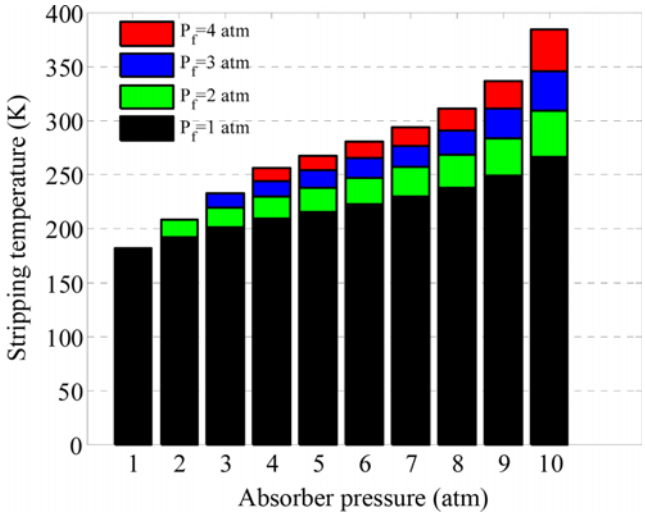

Fig. 14. Effect of absorber and stripper pressure on the recovery temperature at L=CO_2cap/m, f=85%.

served. It is found that the absorber cannot operate at pressure lower than 4 atm as the numerical solution does not provide feasible solution. Fig. 11(c) shows that at P_a=4 atm, the amount of CO_2 in the rich sorbent is almost equal to the amount to be captured at f=85%. Therefore, going below 4 atm, the specified removal efficiency can be attained. In addition, Fig. 12 indicates that the stripping temperature for all pressure values is higher than 300 K and much higher than those reported in the previous simulations. Moreover, the variation of the intended stripping temperature varies marginally with the absorber pressure. The answer for these phenomena is given in Fig. 11, which shows that very small amount of CO_2 is absorbed over the entire range of operating pressure. Therefore, the ratio of the amount of CO_2 to be released in the stripper to the total amount of CO_2 in the stripper feed for all values of the pressure is very high. It should be noted that at the given operating condition and removal efficiency, the amount of CO_2 captured is 510 kmol/h. As discussed earlier, this situation entails elevated energy. Furthermore, the variation of the CO_2 content in the stripper feed over the range of pressure values is minor. Hence, the variation of the needed flashing temperature will also be small over the given range of operating pressure.

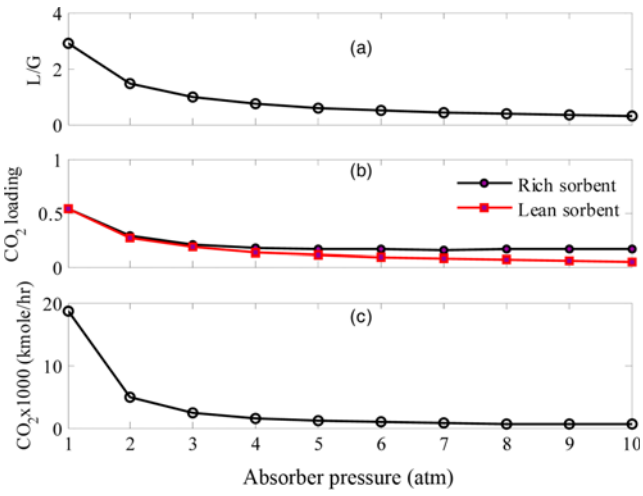

Fig. 13. Effect of pressure on the absorption rate at L=CO_2cap/m, f=85%, T=25 °C.

Finally, the influence of fixing the solvent flow rate on the process performance was investigated. Instead of fixing L randomly, it was taken as the ratio of the amount of CO_2 to be captured to the CO_2 solubility factor: L=CO_2cap/m. The results of this simulation, depicted in Figs. 13 and 14, emphasize the fact that lower absorber pressure values causes unrealistic outcomes. The unique finding is the possibility to attain feasible solution at low absorber pressure of 1 atm. In this situation, the solvent flow rate is allowed to vary with the column pressure via the solubility factor. This will allow the use of huge amount of sorbent at low pressure; consequently, large amount of CO_2, even more than is desired, can be carried out with the solvent.

The interesting finding is that the temperature requirement for this type of IL can be maintained much below 100 °C by adjusting the absorber/stripper operating pressure. For comparison, it is reported that the temperature required for CO_2 capturing using MEA reaches 120 °C even when the stripper is operating as low as 1 atm [5-7,46].

CONCLUSIONS

This work is an attempt to study the use of ILs in a typical CO_2 capturing process. The recovery operation is modeled based on the well-known PR equation of state, which is validated using the experimental solubility of CO_2 in 1-butyl-3-methylimidazolium tetrafluoroborate IL. Parametric investigation is carried out using the developed model to determine the solvent and energy demands to recover specific amount of CO_2 from the flue gas using 1-butyl-3-methylimidazolium tetrafluoroborate. The energy demand is represented by the VLE temperature necessary to emit the captured CO_2 from the spent solvent. The simulation results indicated that the absorber column should run at pressure higher than 8 atm to obtain physically feasible operation. Moreover, the stripper column should operate within 1-2 atm to minimize the energy requirement necessary to regenerate the captured CO_2. In general, the energy require-

ment of the stripper used to flash the CO_2 out of the IL is less than that demanded to separate the captured CO_2 from MEA solvent in the amine-based processes. This finding may not be valid when the energy requirement for the entire process is considered. Furthermore, the energy demand increases as the CO_2 content in the rich sorbent decreases. In other words, the energy needed to release the captured CO_2 in the stripper does not only depend on the CO_2 solubility but also on the amount of CO_2 present in the stripper feed.

LIST OF SYMBOLS

a, b, A, B : parameters of the PR equation of state for pure fluid and mixture
CO_{cap} : amount of CO_2 captured in absorber column
F : molar flow rate of the flash feed
f_i^{π} : fugacity of species I in phase p
G : gas phase flow rate
i, j : component identifiers
K_i : equilibrium constant of component i
k_{ij} : binary interaction parameter between i and j
L : liquid phase flow rate
nc : number of components
P : absolute pressure
P_f : stripper pressure
R : universal gas constant
T : absolute temperature
v : the molar volume
x_i : mole fraction of component i in the liquid phase
x_f : CO_2 loading in the lean solvent
y_i : mole fraction of component i in the vapor phase
z_i : mole fraction of component i in the feed mixture
Z : compressibility factor
λ : ratio of the produced vapour to the feed
ϕ_i^{π} : fugacity coefficient of component i in the phase p

ACKNOWLEDGEMENT

The authors thank the National Plan for Science, Innovation, and Technology at King Saud University for their financial assistance through project no. 10-ENV1010-02.

REFERENCES

1. A. Yamasaki, *J. Chem. Eng. Japan*, **36**(4), 361 (2003).
2. S. M. Cohen, H. L. Chalmers, M. E. Webber and C. W. King, *Environ. Res. Lett.*, **6**, 1 (2011).
3. C. B. Tarun, E. Croiset, P. L. Douglas, M. Gupta and M. H. M. Chowdhury, *Int. J. Greenhouse Gas Control*, **1**, 55 (2007).
4. N. Dave, T. Do, G. Puxty, R. Rowland, P. H. M. Feron and M. I. Attalla, *Energy Procedia*, **1**, 949 (2009).
5. N. Rodriguez, S. Mussati and N. Scenna, *Chem. Eng. Res. Design*, **89**, 1763 (2011).
6. M. Mofarhi, Y. Khojasteh, H. Khaledi and A. Farahnak, *Energy*, **33**, 1311 (2008).
7. M. Abu-Zahra, L. H. Schneides, J. P. Niederer, P. H. Feron and G. F. Versteeg, *Int. J. Greenhouse Gas Control*, **1**, 37 (2007).
8. M. K. Hanne and G. T. Rochelle, *Ind. Eng. Chem. Res*., **47**, 867 (2008).
9. B. R. Anand, E. S. Rubin, D. W. Keith and M. G. Morgan, *Energy Policy*, **34**, 3765 (2006).
10. L. A. Blanchard, D. Hancu, E. J. Beckman and J. F. Brennecke, *Nature*, **399**, 28 (1999).
11. J. Huang and T. Ruther, *Aust. J. Chem.*, **62**, 298 (2006).
12. X. Zhang, H. Dong, Z. Zhao, S. Zhang and Y. Huang, *Energy Environ. Sci*., **5**, 6668 (2012).
13. S. N. V. K. Aki, B. R. Mellein, E. M. Saurer and J. F. Brennecke, *J. Phys. Chem. B*, **108**, 20355 (2004).
14. S. G. Kazarian, B. J. Briscoe and T. Welton, *Chem. Commun*., **20**, 2047 (2000).
15. J. Jacquemin, M. F. Costa Gomes, P. Husson and V. Majer, *J. Chem. Thermodyn*., **38**, 490 (2006).
16. D. Y. Peng and D. B. Robinson, *Ind. Eng. Chem. Fundam.*, **15**(1), 59 (1876).
17. A. H. Harvey, *Application of molecular modeling to vapor-liquid equilibrium of water with synthesis gas*, *15th Inter Conference on the Properties of Water and Steam*, Berlin, Sep. 8-11 (2008).
18. X. C. Tombokan, *Ternary phase equilibrium of the sclareol-ethyl lactate-CO_2 system and its application in the extraction and isolation of sclareol from clary sage*, PhD Dissertation 2008, North Carolina State University, USA.
19. T. Greer, *Modeling and simulation of post combustion CO_2 capturing*, MSc Thesis 2008, Telemark University College, Norway.
20. E. O. Lars, *Aspen HYSYS simulation of CO_2 removal by amine absorption from a gas based power plant*, *The 48th Scandinavian Conference on Simulation and Modeling*, Gøteborg, Oct. 30-31 (2007).
21. M. A. Shiflett and A. Yokozeki, *Ind. Eng. Chem. Res*., **44**, 4453 (2005).
22. F. M. Maia, I. Tsivintzelis, O. Rodriguez, E. A. Macedo and G. M. Kontogeorgis, *Fluid Phase Equilib.*, **332**, 128 (2012).
23. L. F. Vega, O. Vilaseca, F. Llovell and J. S. Andreu, *Fluid Phase Equilib.*, **294**, 15 (2010).
24. V. H. Alvarez and M. Aznar, *J. Chin. Inst. Chem. Eng*., **39**, 353 (2008).
25. P. J. Carvalho, V. H. Álvarez, I. M. Marrucho, M. Aznar and J. A. P. Coutinho, *J. Supercrit. Fluids*, **48**, 99 (2009).
26. P. J. Carvalho, V. H. Álvarez, I. M. Marrucho, M. Aznar and J. A. P. Coutinho, *J. Supercrit. Fluids*, **50**, 105 (2009).
27. J. O. Valderrama, A. Reategui and W. W. Sanga, *Ind. Eng. Chem. Res*., **47**, 8416 (2008).
28. S. Mattedi, P. J. Carvalho, J. A. P. Coutinho, V. H. Alvarez and M. Iglesias, *J. Supercrit. Fluids*, **56**, 224 (2011).
29. J. O. Valderrama, F. Urbina and C. A. Faúndez, *J. Supercrit. Fluids*, **64**, 32 (2012).
30. P. F. Arce, P. A. Robles, T. A. Graber and M. Aznar, *Fluid Phase Equilib*., **295**, 9 (2010).
31. W. Ren, B. Sensenich and A. M. Scurto, *J. Chem. Thermodynamics*, **42**, 305 (2010).
32. J.-H. Yim, H. N. Song, B.-C. Lee and J. S. Lim, *Fluid Phase Equilib.*, **308**, 147 (2011).
33. S. Hwang, Y. Park and K. Park, *J. Chem. Thermodyn*., **43**, 339 (2011).
34. A. Shariati, *J. Supercrit. Fluids*, **25**, 109 (2003).
35. E. K. Shin, B. L. Lee and J. S. Lim, *J. Supercrit. Fluids*, **45**, 282

(2008).
36. H. N. Song, B.-C. Lee and J. S. Lim, *J. Chem. Eng. Data*, **55**, 891 (2010).
37. S. Jang, D.-W. Cho, T. Im and H. Kim, *Fluid Phase Equilib*., **299**, 216 (2010).
38. W. Ren and A. M. Scurto, *Fluid Phase Equilib*., **286**, 1 (2009).
39. S. O. Nwosu, J. C. Schleicher and A. M. Scurto, *J. Supercrit. Fluids*, **51**, 1 (2009).
40. A. L. Revelli, F. Mutelet and J. N. Jaubert, *J. Phys. Chem. B*, **114**, 8199 (2010).
41. A. L. Revelli, F. Mutelet and J. N. Jaubert, *J. Phys. Chem. B*, **114**, 12908 (2010).
42. R. Bogel-Łukasik, D. Matkowska, E. Bogel-Łukasik and T. Hofman, *Fluid Phase Equilib*., **293**, 168 (2010).
43. S. L. Sandler, *Chemical and engineering thermodynamics*, 3rd Ed. Wiley (1999).
44. Z. Nasri and H. Binous, *Chem. Eng. Education*, **43**(2), 1 (2009).
45. J. O. Valderrama, L. A. Forero and R. E. Rojas, *Ind. Eng. Chem. Res.*, **51**(22), 7838 (2012).
46. T. Greer, A. Bedelbayev, J. Igreja, J. Gomrz and B. Lie, *A dynamic model for the de-absorption of carbon dioxide from monoethanolamine solution*, *The 49th Scandinavian Conference on Simulation and Modeling* (SIMS2008), Oslo University, Oct. 7-8 (2008).